JOC Article

Molecular Dynamics Study of [2]Rotaxanes: Influence of Solvation and Cation on Co-conformation

Xavier Fradera,[†,‡] Manuel Márquez,[§] Bradley D. Smith,[||] Modesto Orozco,*[,⊥,#] and F. Javier Luque*[,†]

Departament de Fisicoquímica, Facultat de Farmàcia, Universitat de Barcelona, A. Diagonal 643, 08028 Barcelona, Spain, Chemistry Division, Los Alamos National Laboratory, Los Alamos, New Mexico 87545, Department of Chemistry and Biochemistry, University of Notre Dame, Notre Dame, Indiana 46556-5670, Institut de Recerca Biomédica, Parc Científic de Barcelona, c/. Josep Samitier 1-6, 08028 Barcelona, and Departament de Bioquímica i Biología Molecular, Facultat de Química, Universitat de Barcelona, c/. Martí i Franqués 1, 08028 Barcelona, Spain

javier@far1.far.ub.es; modesto@mmb.pcb.ub.es

Received April 11, 2003

The conformational preference of a [2]rotaxane system has been examined by molecular dynamics simulations. The rotaxane wheel consists of two bridged binding components: a *cis*-dibenzo-18-crown-6 ether and a 1,3-phenyldicarboxamide, and the penetrating axle consists of a central isophthaloyl unit with phenyltrityl capping groups. The influence of solvation on the co-conformation of the [2]rotaxane was evaluated by comparing the conformational flexibility in two solvents: chloroform and dimethyl sulfoxide. Attention was also paid to the effect of cation binding on the dynamical properties of the [2]rotaxane. The conformational stability of the [2]rotaxane was calculated using a MM/PB-SA strategy, and the occurrence of specific motions was examined by essential dynamics analysis. The changes in the co-conformational properties in the two solvents and upon cation binding are discussed in light of the available NMR data. The results indicate that in chloroform solution the [2]rotaxane system exists as a mixture of co-conformational states including some that have hydrogen bonds between axle C═O and wheel NH groups. Analysis of the simulations allow us to hypothesize that the [2]rotaxane's circumrotation motion can occur as the result of a dynamic process that combines a preliminary axle sliding step that breaks these hydrogen bonds and a conformational change in the ester group more distant from the wheel. In contrast, no hydrogen-bonded co-conformation was found in dimethyl sulfoxide, which appears to be due to the preferential formation of hydrogen bonds between the wheel NH groups with solvent molecules. Moreover, the axle experiences notable changes in anisotropic shielding, which would explain why the NMR signals are broadened in this solvent. Insertion of a sodium cation into the crown ether reduces co-conformational flexibility due to an interaction of the axle with the cation. Overall, the results reveal how both solvent and ionic atmosphere can influence the co-conformational preferences of rotaxanes.

Introduction

Rotaxanes are molecules that consist of two noncovalently interlocked components, the wheel and a penetrating dumbell-shaped axle, the latter component bearing stoppers large enough to prevent unthreading of the ring. Topologically, the formation of a rotaxane can be viewed as "mechanical isomerism",[1] where chemical bonds have to be distorted in an imaginary transition from the separate components to the interlocked structure in order to form the mechanical bond (see Scheme 1). From a synthetic point of view, a number of different template-directed synthetic strategies have been reported.[2] In one instance, a linear half-dumbbell-shaped compound is threaded through the cavity of a preformed macrocycle with the assistance of noncovalent bonding interactions and then stoppered by the covalent attachment of a bulky group. In another instance, the macro-

SCHEME 1

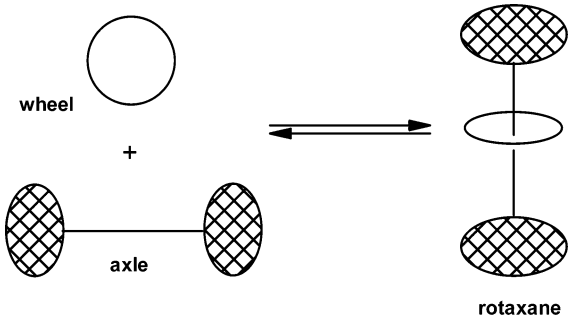

[†] Universitat de Barcelona.
[‡] Present address: Computacional Medicinal Chemistry, Organon Laboratorios Ltd., Newhouse, ML1 5SH Lanarkshire, Scotland, U.K.
[§] Los Alamos National Laboratory.
[||] University of Notre Dame.
[⊥] Parc Científic de Barcelona.
[#] Universitat de Barcelona.

(1) *Molecular Catenanes, Rotaxanes and Knots*; Sauvage, J. P., Dietrich-Bucheker, C. O., Eds.; VCH−Wiley: Weinheim, 1999.

10.1021/jo034457d CCC: $25.00
Published on Web 05/17/2003

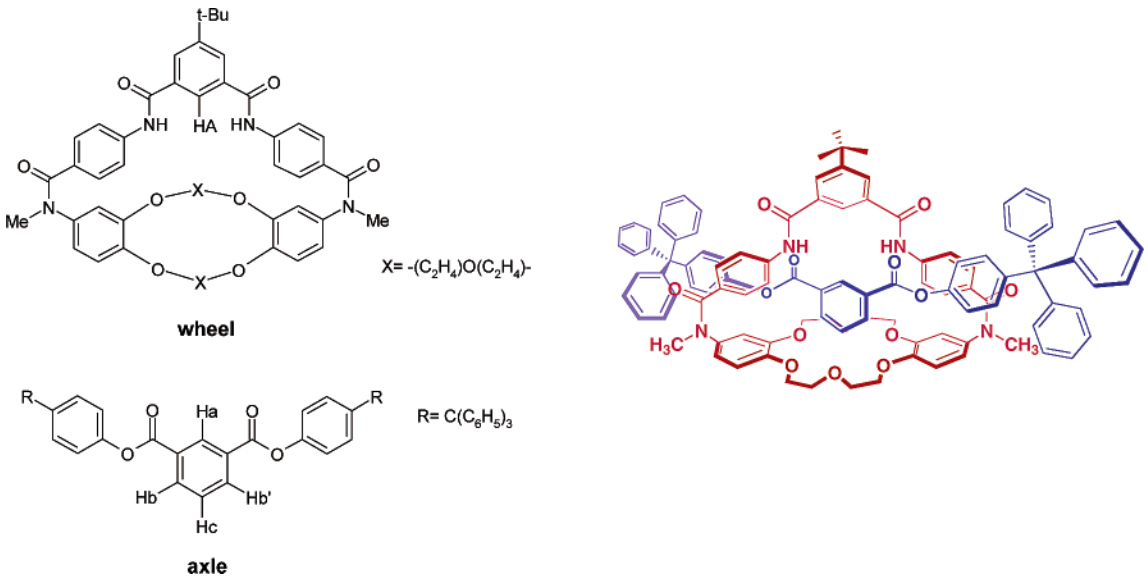

FIGURE 1. Schematic representation of the wheel and axle components and the assembled [2]rotaxane system examined in the study. Two bridged binding systems, a *cis*-dibenzo-18-crown-6 ether unit, and a 1,3-phenyldicarboxamide moiety form a bicyclic wheel. The axle consists of a central isophthaloyl diester linked to two phenyltrityl capping groups.

cycle is clipped around the preformed dumbbell. Finally, an alternative approach is provided by slippage, where the separate macrocycle and dumbbell-shaped components are heated together in solution and the macrocycle "slips" over the dumbbell's stoppers.

Rotaxanes are of current interest as model systems for molecular recognition and for their potential biotechnological applications, particularly as precursors for artificial molecular machines. To this end, the molecular elements of rotaxanes have to be assembled in a coherent manner and their motion controlled by means of specific structural devices. Rotaxanes can exhibit a number of dynamical features, such as *shuttling* or *pirouetting*, which denote the motion of the wheel sliding along or rotating around the axle, respectively (since this latter motion has also been used to describe the interconversion of inner-to-outer ring isomers within catenane,[3] here we use the term "circumrotation" to avoid any potential confusion). Unthreading (i.e., the loss of the axle from the wheel) might also be possible, though this is synthetically prevented by attaching suitable capping groups to the axle. The incorporation of specific functional groups into suitably preorganized scaffolds allows control of rotaxane dynamics by means of switching strategies based on chemical effectors, such as protons,[2g,4] metal cations,[5] anions,[6] and amines.[7] Switching strategies that exploit photochemical and electrochemical properties of rotaxane elements have also been investigated.[4a,8] Characterization of the dynamical behavior of rotaxanes is of fundamental importance for their biotechnological application.

This study is focused on a [2]rotaxane system with cation-dependent switchable properties[9−11] (see Figure 1). The wheel consists of two bridged binding systems: a *cis*-dibenzo)-18-crown-6 ether unit and a 1,3-phenyldicarboxamide moiety. The axle consists of a central isophthaloyl unit linked to phenyltrityl capping groups.

Knowledge of the structural features of the [2]rotaxane in solution is largely facilitated by NMR techniques. The ^{1}H NMR signals of the axle isophthalate protons reveals that the symmetry of the axle is altered upon formation of the [2]rotaxane. For instance, the protons H_b (see Figure 1), which give a signal at 8.43 ppm when free in chloroform solution, are no longer chemically equivalent when incorporated into the rotaxane, where two doublets at 8.64 and 8.55 ppm are observed.[11] Moreover, the room-temperature ^{1}H NMR spectrum of the rotaxane in chloroform is well resolved and exhibits no dynamic behavior after cooling, which can be ascribed to the predominance of a specific co-conformation (i.e., the relative orientation of the component parts of an interlocked molecule). In contrast, the ^{1}H NMR spectrum of

(2) (a) Reuter, C.; Wienand, W.; Hübner, G. M.; Seel, C.; Vögtle, F. *Chem. Eur. J.* **1999**, 5, 2692. (b) Raymo, F.; Stoddart, J. F. *Chem. Rev.* **1999**, *99*, 1643. (c) Hübner, G.; Gläser, J.; Seel, C.; Vögtle, F. *Angew. Chem., Int. Ed. Engl.* **1999**, *38*, 383. (d) Seel, C.; Vögtle, F. *Chem. Eur. J.* **2000**, *6*, 21. (e) Mahoney, J. M.; Shukla, R.; Marshall, R. A.; Zajicek, J.; Beatty, A. M.; Smith, B. D. *J. Org. Chem.* **2002**, *67*, 1436−1440.

(3) Ashton, P. R.; Ballardini, R.; Balzani, V.; Gandolfi, M. T.; Marquis, D. J.-F.; Pérez-García, L.; Prodi, L.; Stoddart, J. F.; Venturi, M. *J. Chem. Soc., Chem. Commun.* **1994**, 177.

(4) (a) Balzani, V.; Credi, A.; Raymo, F. M.; Stoddart, J. F. *Angew. Chem., Int. Ed.* **2000**, *39*, 3348. (b) Anelli, Spencer, N.; Stoddart, J. F. *J. Am. Chem. Soc.* **1991**, *113*, 5131. (c) Sauvage, J. P. *Acc. Chem. Res.* **1998**, *31*, 611.

(5) (a) Asakawa, M.; Ashton, P. R.; Iqbal, S.; Stoddart, J. F.; Tinker, N. D.; White, A. J. P.; Williams, D. J. *Chem. Commun.* **1996**, 483. (b) Amabilino, D. B.; Dietrich-Buchecker, C. O.; Livoreil, A.; Pérez-García, L.; Sauvage, J. P.; Stoddart, J. F. *J. Am. Chem. Soc.* **1997**, *119*, 12114. (c) Fyfe, M. C. T.; Glink, P. T.; Menzer, S.; Stoddart, J. F.; White, A. J. P.; Williams, D. J. *Angew. Chem., Int. Ed. Engl.* **1997**, *36*, 2068.

(6) (a) Montalti, M.; Prodi, L. *Chem. Commun.* **1998**, 1461. (b) Andrievsky, A.; Ahuis, F.; Sessler, J. L.; Vögtle, F.; Gudat, D.; Moini, M. *J. Am. Chem. Soc.* **1998**, *120*, 9712.

(7) Balzani, V.; Credi, A.; Langford, S. J.; Raymo, F. M.; Stoddart, J. F.; Venturi, M. *J. Am. Chem. Soc.* **2000**, *122*, 3542.

(8) (a) Wong, E. W.; Collier, C. P.; Belohradsky, M.; Raymo, F. M.; Stoddart, J. F.; Heath, J. R. *J. Am. Chem. Soc.* **2000**, *122*, 8531. (b) Brouwer, A. M.; Frochot, C.; Gattiu, F. G.; Leigh, D. A.; Mottier, L.; Paolucci, F.; Roffia, S.; Wirpel, G. W. H. *Science* **2001**, *291*, 2124.

(9) Deetz, M. J.; Shang, M.; Smith, B. D. *J. Am. Chem. Soc.* **2000**, *122*, 6201.

(10) Shukla, R.; Deetz, M. J.; Smith, B. D. *Chem. Commun.* **2000**, 2397.

(11) Deetz, M. J.; Shukla, R.; Smith, B. D. *Tetrahedron* **2002**, *58*, 799.

the rotaxane in dimethyl sulfoxide (DMSO) shows broad signals for the axle protons at room temperature, which nevertheless sharpen considerably upon addition of 5 molar equiv of KPF_6.

This theoretical study uses molecular dynamics (MD) simulations to build a precise molecular description of the co-conformational flexibility of the [2]rotaxane system in chloroform and DMSO. In particular, attention is focused on the most likely structure of the free [2]-rotaxane in these solvents and how this information can be used to interpret the differences in ^{1}H NMR spectra. Another interesting issue is the effect of the KPF_6 salt on the co-conformational preference of the [2]rotaxane in DMSO. The results provide insight into the noncovalent factors that control rotaxane co-conformation.

Methods

Quantum Mechanical Calculations. The intrinsic conformational preferences of the axle were explored by quantum mechanical (QM) calculations carried out for a model compound where the (triphenyl)methylbenzene units attached to the isophthaloyl diester moiety were replaced by methyl groups. Three different conformations differing in the relative orientation of the two ester groups were considered. In each case, the geometry was fully optimized at the Hartree−Fock[12] (HF) level with the 6-31G(d) basis set,[13] and the minimum energy nature of the stationary points was confirmed by the positive values of the harmonic vibrational frequencies. Single-point calculations were performed at the B3LYP/6-31G-(d)[14] level using the HF/6-31G(d)-optimized geometries. Zero-point energy and thermal and entropic corrections (at 1 atm and 298 K standard reference state) were determined from the HF/6-31G(d) vibrational frequencies scaled by a factor of 0.893[15] and using the harmonic oscillator−rigid rotor models as implemented in Gaussian-98.[16] The relative stability in the gas phase was determined by adding thermal and entropic corrections to the B3LYP/6-31G(d) energy differences.

To investigate the effect of solvation on the relative stability of the axle, self-consistent reaction field computations were performed to determine the free energies of solvation in chloroform, DMSO, and water by using the MST[17] continuum model. For calculations in DMSO, the differences in the free energy of solvation were determined by considering only the electrostatic component, which was computed by scaling the van der Waals radii by a factor of 1.40.[18] This approximation is justified by the cancellation of the nonelectrostatic term when the solvation free energies determined for the different conformations of the model compound in either chloroform or water were compared.

Molecular Dynamics Calculations. Molecular dynamics (MD) simulations were performed to explore the conformational space of the rotaxane. In particular, attention was paid to examine how changes in the solvent and the presence of cations might influence the co-conformational preferences of rotaxanes and to whether the natural dynamics of rotaxanes might explain typical motions such as circumrotation.

All the simulations described here were performed using the AMBER6 suite of programs.[19] For the rotaxane, bonded and van der Waals parameters were adopted from the values implemented for similar groups in the standard AMBER-95 force field.[20] The atomic point charges were determined using the RESP[21] procedure at the HF/6-31G(d) level. RESP charges were derived separately for the dibenzo-18-crown-6 ether and 1,3-phenyldicarboxamide moieties of the wheel and for the isophthaloyl diester and phenyltrityl units of the axle. Neutrality was imposed by slight adjustments of point charges on the *N*-methyl groups in the wheel and on the trityl stopper groups of the axle. Chloroform and DMSO were represented as solvents by using the OPLS force field.[22]

The model system of the rotaxane in solution was generated by using the standard rules defined in AMBER for addition of previously Monte Carlo-equilibrated boxes of chloroform and DMSO solvents. The final systems consisted of a roughly cubic box of around 35 000 Å^3. Different starting co-conformations were considered for the free rotaxane in chloroform and in DMSO (see below). Subsequent MD simulations involved a total production simulation time of nearly 0.1 μs.

In all cases, the starting system was energy-minimized for 4000 (1000 steepest-descent + 3000 conjugate gradient) cycles to release unfavorable contacts and followed by 100 ps MD run where the temperature was raised in five steps (each 20 ps) keeping the temperature at values of 100, 150, 200, and 250 at 298 K, respectively. The relative orientation of the axle in the wheel defined in the starting conformation was maintained by imposing suitable restraints, which were eliminated in a subse-

(12) Hehre, W. J.; Radom, L.; Schleyer, P. v. R.; Pople, J. A. *Ab Initio Molecular Orbital Theory*; John Wiley & Sons: New York, 1986.
(13) Hariharan, P. C.; Pople, J. A. *Theor. Chim. Acta* **1973**, *28*, 213.
(14) (a) Becke, A. D. *J. Chem. Phys.* **1993**, *98*, 5648. (b) Lee, C.; Yang, W.; Parr, R. G. *Phys. Rev. B* **1988**, *37*, 785.
(15) Hout, R. F.; Leri, B. A.; Hehre, W. J. *J. Comput. Chem.* **1982**, *3*, 234.
(16) Frisch, M. J.; Trucks, G. W.; Schlegel, H. B.; Scuseria, G. E.; Robb, M. A.; Cheeseman, J. R.; Zakrzewski, V. G.; Montgomery, J. A.; Stratmann, R. E.; Burant, J. C.; Dapprich, S.; Millam, J. M.; Daniels, A. D.; Kudin, K. N.; Strain, M. C.; Farkas, O.; Tomasi, J.; Barone, V.; Cossi, M.; Cammi, R.; Mennucci, B.; Pomelli, C.; Adamo, C.; Clifford, S.; Ochterski, J.; Petersson, G. A.; Ayala, P. Y.; Cui, Q.; Morokuma, K.; Salvador, P.; Dannenberg, J. J.; Malick, D. K.; Rabuck, A. D.; Raghavachari, K.; Foresman, J. B.; Cioslowski, J.; Ortiz, J. V.; Baboul, A. G.; Stefanov, B. B.; Liu, G.; Liashenko, A.; Piskorz, P.; Komaromi, I.; Gompets, R.; Martin, R. L.; Fox, D. J.; Keith, T.; Al-Laham, M. A.; Peng, C. Y.; Nanayakkara, A.; Challacombe, M.; Gill, P. M. W.; Johnson, B.; Chen, W.; Wong, M. W.; Andres, J. L.; Gonzalez, C.; Head-Gordon, M.; Replogle, E. S.; Pople, J. A. *Gaussian-98*; Gaussian, Inc.: Pittsburgh, PA, 2001.
(17) (a) Curutchet, C.; Orozco, M.; Luque, F. J. *J. Comput. Chem.* **2001**, *22*, 1180. (b) Luque, F. J.; Zhang, Y.; Alemán, C.; Bachs, M.; Gao, J.; Orozco, M. *J. Phys. Chem.* **1996**, *100*, 4269. (c) Bachs, M.; Luque, F. J.; Orozco, M. *J. Comput. Chem.* **1994**, *15*, 446.
(18) Curutchet, C.; Orozco, M.; Luque, F. J. Unpublished results.
(19) Case, D. A.; Pearlman, D. A.; Caldwell, J. W.; Cheatham, T. E., III; Ross, W. S.; Simmerling, C. L.; Darden, T. L.; Marz, K. M.; Stanton, R. V.; Cheng, A. L.; Vincent, J. J.; Crowley, M.; Tsui, V.; Radmer, R. J.; Duan, Y.; Pitera, J.; Massova, I.; Seibel, G. L.; Singh, U. C.; Weiner, P. K.; Kollman, P. A. *AMBER6*; University of California: San Francisco, 1999.
(20) Cornell, W. D.; Cieplak, P.; Bayly, C. I.; Gould, I. R.; Merz, K.; Ferguson, D. M.; Spellmeyer, D. C.; Fox, T.; Caldwell, J. W.; Kollman, P. A. *J. Am. Chem. Soc.* **1995**, *117*, 5179.
(21) Bayly, C. I.; Cieplak, P.; Cornell, W. D.; Kollman, P. A. *J. Phys. Chem.* **1993**, *97*, 10269.
(22) (a) Jorgensen, W. L.; Briggs, J. M.; Contreras, L. *J. Phys. Chem.* **1990**, *94*, 163. (b) Jorgensen, W. L. BOSS version 4.2 computer program, Yale University, 2000.

quent 100 ps MD run at 298 K. Then, a production MD simulation was performed at constant temperature and pressure (298 K and 1 atm) for a total simulation time of 8 ns, though in some cases it was enlarged up to 20 ns. Periodic boundary conditions, particle-mesh Ewald method for electrostatic interactions, and a 12 Å nonbonded cutoff for van der Waals interactions were used. SHAKE[22] was adopted to maintain bond lengths at their equilibrium values, which allowed us to use an integration time step of 2 fs.

The influence of cation-binding on the rotaxane dynamics was examined for selected co-conformations of the rotaxane (see below). To this end, a Na^+ cation was placed in the crown ether and the system was solvated as noted above. Neutrality of the whole system was maintained by replacing a molecule of the solvent by a chloride anion. Heating and equilibration was performed by using the protocol mentioned above. The position of the cation in the crown was fixed by suitable restrains along the MD simulation.

Essential Dynamics Study. MD trajectories were analyzed using principal component analysis (PCA) to explore the natural motions of the rotaxane. To this end, covariance matrices were built up from the collected snapshots and diagonalized to obtain both eigenvalues and eigenvectors, which were analyzed to extract information about the frequency and the nature of the structural fluctuations in the rotaxane.

The occurrence of a given motion (i.e., circumrotation) can be quantitatively measured from the similarity index α_k ($0 \le \alpha_k \le 1$) given in eq 1, where $\bar{\omega}$ denotes the transition vector associated to that motion and $\bar{\gamma}_k$ stands for the eigenvector related to mode k. Equation 1 can be generalized to a given subset of essential modes, as shown in eq 2, leading to a global similarity index, β. For our purposes, the index β was determined by considering the three principal modes, which account for more than 50% of the total structural variance of the rotaxane in the trajectories collected in chloroform and DMSO.

$$\alpha_k = \bar{\omega} \cdot \bar{\gamma}_k \tag{1}$$

$$\beta = \sum_{k=1}^{N} (\bar{\omega} \cdot \bar{\gamma}_k)^2 \tag{2}$$

where N denotes the number of essential modes included in the subset.

Energetic Analysis. To investigate the conformational preferences of the rotaxane system, an MM/PBSA strategy was used to analyze 300 snapshots collected regularly along 3 ns MD simulation for each of the co-conformations examined in the MD simulations. In general, the analyzed trajectory corresponded to the 5−8 ns portion of the MD run, but other 3 ns windows were occasionally also examined (see below). In all cases, those windows were chosen so that the positional root-mean-square deviation showed no drastic fluctuations.

The intramolecular energy components (averaged for the selected snapshots) of the rotaxane system were computed by using the AMBER95 force-field with no cutoff for nonbonded interactions. The electrostatic interaction with the solvent was determined from continuum solvation calculations. The solute/solvent interface was defined by using the atomic van der Waals radii defined in the AMBER95 force field and a probe sphere having a radius of 2.5 for the two solvents. Partial charges on the rotaxane were taken from the AMBER95 force field. A dielectric permittivity of 1 was assigned to the cavity that enclosed the rotaxane. The solvent dielectric was set to 4.7 and 47.2 for chloroform and DMSO. The electrostatic component of the solvation energy was determined by solving the Poisson equation by using the MEAD program.[24] A focusing strategy was used to determine the electrostatic free energy of solvation, the finest cubic grid having 0.5 Å spacing and an edge dimension of 61 Å. The nonpolar component of the free energy of solvation was determined by using a term dependent on the solvent-accessible surface, which was determined by using the SURFPDB program.[25] The nonelectrostatic term of the solvation free energy was determined by scaling the solvent-accessible surface by surface tersions of 10.3 and 5.6 cal mol^{-1} $Å^{-1}$ for chloroform and DMSO, which were derived from empirical fitting between the free energies of solvation and solvent-accessible surfaces of alkanes in the two solvents.[26] Though the total contribution of the nonpolar term is significant, the exposed surface area was found to vary little between the different co-conformations of the rotaxane, which suggests that this component is expected to have little effect on the relative stability.

Entropy Calculations. Theoretical estimation of the configurational entropy is difficult for very flexible molecules, since simulation times are too short to allow a complete exploration of the accessible configurational space as well as to deviations from the harmonic (or *quasi*-harmonic) behavior. Accordingly, to reduce the statistical noise, configurational entropies were determined by using Schlitter's method[27] by using a common 3 ns trajectory length for all the representative structures examined here. This method, which has been extensively used by Schafer et al.[28] to examine the conformational preferences of a variety of peptides, relies on the diagonalization of the Cartesian coordinate covariance matrix of the collected snapshots (300 snapshots collected every 10 ps along 3 ns windows). In all cases, the 3 ns windows corresponded to equilibrium trajectories, where no large conformational fluctuations were found. Moreover, contributions due to the *tert*-butyl groups in the wheel and the capping groups of the axle were omitted to further reduce the uncertainty due to spurious contributions arising from these groups. Finally, since the plot of entropy versus the window width exhibited an asymptotic behavior in all cases, the limiting entropy value (S_∞) was determined by fitting the entropies calculated for a range of windows comprised between 0.01 and 3 ns (see eq 3, where τ is an adjustable parameter and t is the simulation time). This approach has been previously used by

(23) Ryckaert, J. P.; Ciccotti, G.; Berendsen, H. J. C. *J. Comput. Phys.* **1977**, *23*, 327.
(24) Bashford, D.; Gewert, K. *J. Mol. Biol.* **1992**, *224*, 473.
(25) Tirado-Rives, J. SURFPDB program, Yale University, 2000.
(26) Experimental data taken from the compilation reported in: Li, J.; Zhu, T.; Hawkins, G. D.; Winget, P.; Liotard, D. A.; Cramer, C. J.; Truhlar, D. G. *Theor. Chem. Acc.* **1999**, *103*, 9.
(27) Schlitter, J. *Chem. Phys. Lett.* **1993**, *215*, 617.
(28) (a) Schafer, H.; Mark, A. E.; van Gunsteren, W. F. *J. Chem. Phys.* **2000**, *113*, 7809. (b) Schafer, H.; Daura, X.; Mark, A. E.; van Gunsteren, W. F. *Proteins* **2001**, *43*, 45.

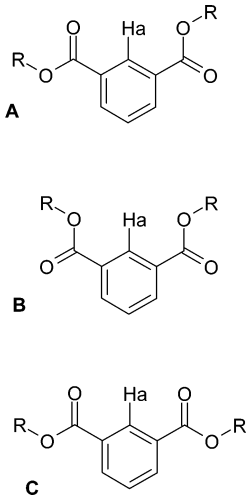

FIGURE 2. Selected conformations of the isophthaloyl diester moiety of the axle.

our own group to study cooperative effects in the binding of drugs to DNA.[29]

$$S(t) = S_\infty - \frac{\tau}{t^{2/3}} \qquad (3)$$

Results and Discussion

Conformation of the Axle. The co-conformational features of the [2]rotaxane are largely modulated by the intrinsic flexibility of the axle and the mechanical constrains imposed by noncovalent interactions between wheel and axle. Besides the rotation of the capping groups, the conformational flexibility of the axle is mainly determined by the relative arrangement of the ester groups bound to the central isophthaloyl ring, giving rise to three basic conformations shown for the model compound dimethyl isophthalate in Figure 2. The two carbonyl groups adopt a trans orientation in conformation A, but a cis arrangement in conformations B and C. These two latter conformations differ in the orientation of the carbonyl groups relative to the hydrogen Ha (anti and syn in conformations B and C, respectively). The relative stabilities of the three conformers in the gas phase and in solution (chloroform, DMSO, and water) are given in Table 1. Conformer C, which is slightly destabilized in the gas phase relative to the other two conformers, is stabilized as the permittivity of the solvent is enlarged. This finding can be explained by the larger charge separation of conformer C compared to that of conformers A and B (see Table 1). Nevertheless, the difference in stability between conformations A, B, and C is small (∼0.5 kcal/mol), and the three conformers of the isophthaloyl diester moiety are expected to be populated both in the gas phase and in solution.

Rotaxane in Chloroform Solution. To investigate the co-conformational preference of the rotaxane, different models of the wheel−axle system were considered (see Figure 3). In all these models, one of the carbonyl oxygens was placed at hydrogen-bonded distance from the wheel NH groups, as can be inferred from the

(29) Harris, S. A.; Gavathiotis, E.; Searle, M. S.; Orozco, M.; Laughton, C. A. *J. Am. Chem. Soc.* **2001**, *123*, 12658.

TABLE 1. Relative Stabilities (kcal/mol; Plain) and Dipole Moments (Debyes; Italics) between Selected Conformations of the Isophthaloyl Diester Moiety in the Gas Phase and in Chloroform (CHL), Dimethyl Sulfoxide (DMSO), and Water (WAT) Solution[a]

conformation	ΔG_{gas}	ΔG_{CHL}	ΔG_{DMSO}	ΔG_{WAT}
A	0.0	0.0	0.0	0.0
	2.02	*2.34*	*2.68*	*3.02*
B	−0.1	0.0	0.0	0.0
	2.37	*2.57*	*2.73*	*2.77*
C	+0.4	+0.1	−0.1	−0.2
	4.02	*4.69*	*5.40*	*6.11*

[a] Free energy differences in solution determined by adding the B3LYP/6-31G(d) free energy differences in the gas phase to the relative values of the free energies of solvation calculated from MST computations. The dipole moments are determined at the HF/6-31G(d) level.

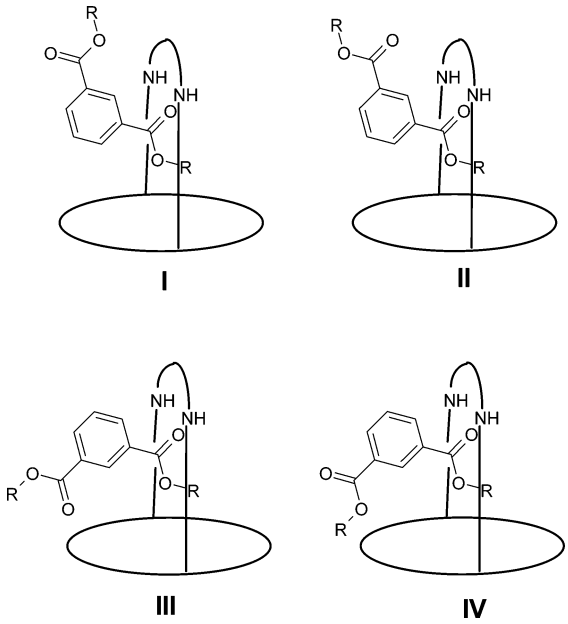

FIGURE 3. Schematic representations of the different rotaxane models **I**−**IV**.

experimental finding that the axle proton H_a interacts through-space with the wheel NH residues and with the wheel proton H_A (see Figures 1 and 3).[11] This restriction is fully accomplished in models **I** and **II**, but not in models **III** and **IV**, which nevertheless were also examined to check the consistency of the MM/PB-SA energetic analysis.

Models **I**−**IV** were used as starting structures for a series of MD simulations (see Methods). The RMSD profiles for the MD trajectories of models **I** and **II** are shown in Figure 4. For model **I** the RMSD profiles show two plateau regions for the windows [1−4] and [5−8] ns separated by a sharp transition that lasts for around 0.5 ns. In the case of model **II**, after the first 7 ns, a series of succesive fluctuations occur along the next 4 ns, leading to a plateau region that persists until the end of the simulation. The RMSD profiles determined for the axle and the wheel suggest that different structural transitions are involved in the two MD trajectories (see below). With regard to models **III** and **IV**, the RMSD profiles revealed no remarkable structural fluctuation along the trajectory (data not shown).

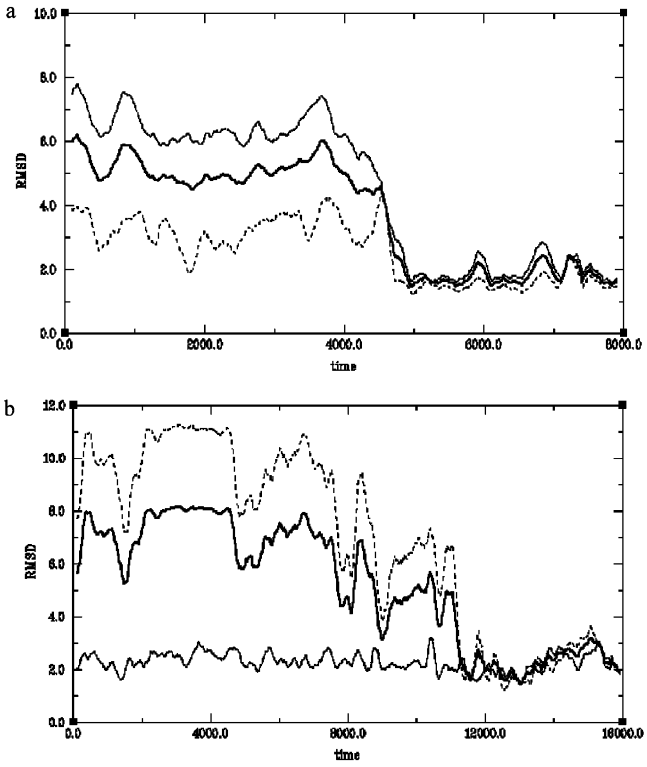

FIGURE 4. Representation of the heavy-atom positional root-mean-square deviation (RMSD; Å) along the trajectories (ps) collected for models (a) **I** and (b) **II** in chloroform for the rotaxane system (solid) and the axle (dotted) and wheel (dashed) components. The RMSD was calculated by fitting the isophthaloyl unit of the axle. Contributions arising from the capping groups of the axle and *tert*-butyl groups in the wheel were not considered to reduce the statistical noise due to their fluctuations. Values determined by using the snapshots at 5 (**I**) and 13 ns (**II**) as reference structures.

Principal component analysis (PCA) was used to examine the essential dynamics of the rotaxane models. Inspection of the first principal modes allowed us to identify a *partial circumrotation* motion only for model **II**. The occurrence of such motion can be measured quantitatively by means of the similarity index (β) defined in eq 3 (see Methods), whose values for the different trajectories are given in Table 2. The β index amounts to 0.44 for model **II**, but it is close to 0 for the rest of models. The structural transition observed in the RMSD profile of model **I** corresponds to a reorientation of the side chain of the axle in the *endo*-face of the wheel isophthalamide bridge, yielding a near-specular image of the rotaxane (see Figure 5a,b). In contrast, the circumrotation motion found for model **II** makes the axle rotate approximately 90° around the wheel (see Figure 5c,d). Even though the completion of a whole circumrotation motion would require a much longer time scale than that explored in present MD simulations, these results indicate that the natural fluctuations of the rotaxane model **II** intrinsically account for the occurrence of such a motion. However, the experimental data indicates that if circumrotation occurs in chloroform, then it must be very fast on the NMR time scale.

The different nature of the structural transitions found for models **I** and **II** appears to be related to the hydrogen-bonding pattern between axle and wheel. Thus, whereas

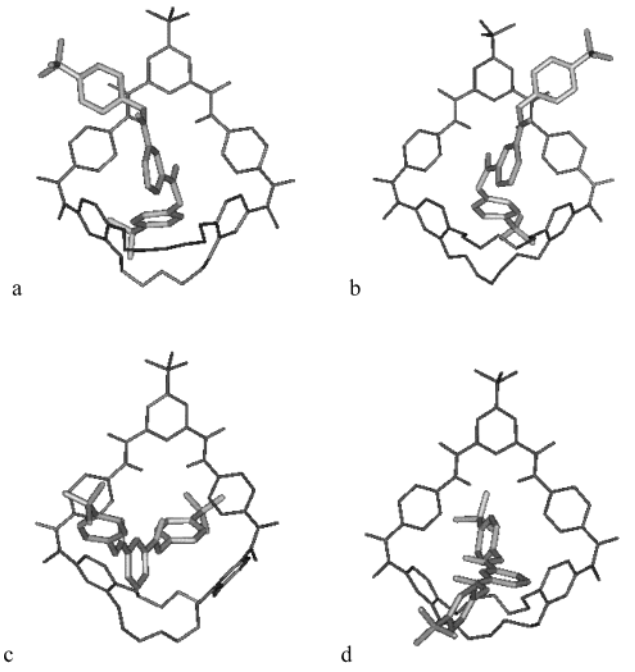

FIGURE 5. Representation of the snapshots collected at (a) 1 and (b) 5 ns for the trajectory of model **I** and at (c) 4 and (d) 13 ns for the trajectory of model **II** in chloroform. For the sake of clarity, the capping groups of the axle and most of the hydrogens atoms are omitted.

a weak hydrogen bond between the axle C═O and wheel NH groups exists in the two windows analyzed for model **I** (average (N)H···O and (N′)H···O distances of 2.73−2.81 Å), those hydrogen-bond contacts are not significantly observed in the two windows examined for model **II** (average (N)H···O and (N′)H···O distances greater than 3.8 Å). In fact, after the partial circumrotation motion in model **II**, the axle C═O group points toward the hydrogens of one of the aryl rings attached to the 1,3-phenyldicarboxamide unit (see Figure 5d), and these (aryl)H···O═C contacts remain stable along the [13−16] ns window. The lack of hydrogen bonding between the axle C═O and wheel NH groups, nevertheless, does not suffice to justify the occurrence of circumrotation motions, because such hydrogen-bonds are also absent in models **III** and **IV** (average (N)H···O and (N′)H···O distances greater than 4.1 Å in the [5−8] ns windows). The adoption of crowded structures for the rotaxane in these latter models inhibits structural fluctuations in the axle. In contrast, the relative motion of the axle and wheel components in model **II** is sterically less hindered because the axle is roughly oriented along the normal to the wheel (Figure 5c,d).

A structural and energetic analysis of the different models was performed for a series of representative co-conformations taken from 3 ns windows where the RMSD remained stable and without large fluctuations. On the basis of the RMSD profiles, six 3 ns windows were considered: [1−4] and [5−8] ns for **I**, [4−7] and [13−16] ns for **II**, and [5−8] ns for both **III** and **IV**. Table 2 reports the heavy-atom positional *self* RMSD values, which measure the structural fluctuation in the set of snapshots collected for each 3 ns window. These values typically amount to around 2.0 Å (for the sake of comparison, the *cross* RMSD values obtained by comparing the structures

TABLE 2. Global Similarity Index, Heavy-Atom Positional Root-Mean-Square Deviations[a] (Å), and Energy Analysis[b] (kcal/mol) for the Snapshots Collected in the Different Simulations of the Rotaxane Models I−IV in Chloroform.

model	I		II		III	IV
			Global Similarity Index			
β	0.05		0.44		0.01	0.02
			RMSD			
	[1−4] ns	[5−8] ns	[4−7] ns	[13−16] ns	[5−8] ns	[5−8] ns
whole	**3.0**	**1.7**	**3.0**	**2.3**	**1.9**	**2.0**
axle/wheel	4.0/2.1	1.9/1.5	1.8/3.6	2.3/2.4	1.8/2.0	2.4/1.8
			Energy Analysis			
E_{axle}	115.7		118.5		118.2	118.3
	0.0		*+2.8*		*+2.5*	*+2.6*
E_{wheel}	178.3		178.8		178.0	178.6
	0.0		*+0.5*		*−0.3*	*+0.3*
$E_{axle-wheel}$						
vdW	−34.4		−29.7		−29.7	−31.6
ele	−2.7		+0.3		−0.6	−0.4
total	−37.1		−29.4		−30.3	−32.0
	0.0		*+7.7*		*+6.8*	*+5.1*
$\Delta \boldsymbol{E}_{\mathbf{rotaxane}}$[c]	*0.0*		*+11.0*		*+9.0*	*+8.0*
$\Delta G_{s,ele}$	−14.2		−15.4		−14.5	−14.9
	0.0		*−1.2*		*−0.3*	*−0.7*
$\Delta G_{s,n-ele}$	−19.5		−20.9		−21.1	−20.5
	0.0		*−1.4*		*−1.6*	*−1.0*
$\Delta\Delta \boldsymbol{G}_{\mathbf{s,total}}$[d]	*0.0*		*−2.6*		*−1.9*	*−1.7*
$-TS_{\infty}$	−106.7		−113.4		−105.1	−105.7
	0.0		*−6.7*		*+1.6*	*+1.0*
$\Delta \boldsymbol{G}_{\mathbf{chl}}$[e]	*0.0*		*+1.7*		*+8.7*	*+7.3*

[a] The RMSD for the whole rotaxane is given in bold, and the separate contributions due to axle (left) and wheel (right) are given in plain text. In all cases, comparison is made with regard to the first snapshot of the 3 ns trajectory used for data collection. The superposition was performed by fitting the isophthaloyl unit of the axle, which showed no conformational change in all cases. No contributions due to the *tert*-butyl in the wheel and the capping groups of the axle were considered. [b] Relative values are given in italics using model **I** as the reference system. Average values were determined for 300 snapshots collected every 10 ps along 3 ns of the trajectory. [c] $E_{rotaxane} = E_{axle} + E_{wheel} + E_{axle-wheel}$. [d] $\Delta G_{s,total} = \Delta G_{s,ele} + \Delta G_{s,n-ele}$. [e] $\Delta G_{chl} = \Delta E_{rotaxane} + \Delta\Delta G_{s,total} - T\Delta S_{\infty}$. The relative stability was determined by using a temperature of 298 K.

sampled in the two 3 ns windows examined for either model **I** or **II** amount to around 6 Å). The wheel is quite rigid, as noted in RMSD values less than 1 Å obtained by superposition of the wheel alone. Therefore, the RMSD values reflect small amplitude thermal fluctuations arising from changes around the C(═O)-O and O−C(aryl) bonds of the axle (note that the RMSD values do not include contributions due to the capping groups) and the co-conformation of the rotaxane.

To examine the relative stability of the co-conformations sampled for models **I**−**IV**, MM/PB-SA calculations (see Methods) were performed. The results are given in Table 2, which reports the average values of the (i) the internal of the axle (E_{axle}) and wheel (E_{wheel}) and the interaction energy between axle and wheel ($E_{axle-wheel}$), which defines the internal energy of the rotaxane ($E_{rotaxane}$); (ii) the electrostatic ($\Delta G_{s,ele}$) and nonelectrostatic ($\Delta G_{s,n-ele}$) components of the solvation free energy ($\Delta G_{s,total}$) of the rotaxane; and (iii) the configurational entropy ($-TS_{\infty}$).

According to the internal energy of the rotaxanes, model **I** is favored by more than 8.0 kcal/mol compared to the rest of models. The larger stability of model **I** stems from (i) the intramolecular energy of the axle (near 3 kcal/mol) and (ii) the intermolecular interaction between axle and wheel (between 5 and 8 kcal/mol), which is largely due to the van der Waals energy. The structures sampled in model **I** are worse solvated (by around 2 kcal/mol) than those collected for the other models, thus reflecting the typical compensation effect between the internal energy of the rotaxane and its solvation free energy. Most of the difference in the solvation free energy is explained by contributions related to the solvent-exposed surface of the rotaxane. Finally, the configurational entropy term favors model **II**, as expected from the sterically less hindered orientation of the axle.

The free energy differences in chloroform (ΔG_{chl}) were estimated from eq 4, where $\Delta E_{rotaxane}$, $\Delta\Delta G_{s,total}$ and $T\Delta S_{\infty}$ stand for the contributions arising from the internal energy, the solvation free energy and the configurational entropy of the rotaxane models. The ΔG_{chl} values reported in Table 2 indicates that the hydrogen-bonded co-conformation (model **I**) is expected to be the main co-conformation, though other co-conformations lacking the specific hydrogen bonding between axle C═O and wheel NH groups (model **II**) might also be populated. Moreover, the results predict that models **III** and **IV** are markedly less stable than model **I** and their occurrence can be ruled out, which agrees with the available experimental evidence.[11]

$$\Delta G_{chl} = \Delta E_{rotaxane} + \Delta\Delta G_{s,total} - T\Delta S_{\infty} \qquad (4)$$

On the basis of the preceding results, the [2]rotaxane system in chloroform at room temperature is expected to exist as an equilibrium between co-conformations with and without hydrogen bonding between the axle C═O and wheel NH groups. Moreover, while the internal energy favors the hydrogen-bonded co-conformation (**I**), the structures without such hydrogen-bonding (**II**) are favored entropically. Therefore, the [2]rotaxane system is expected to be trapped in the hydrogen-bonded co-

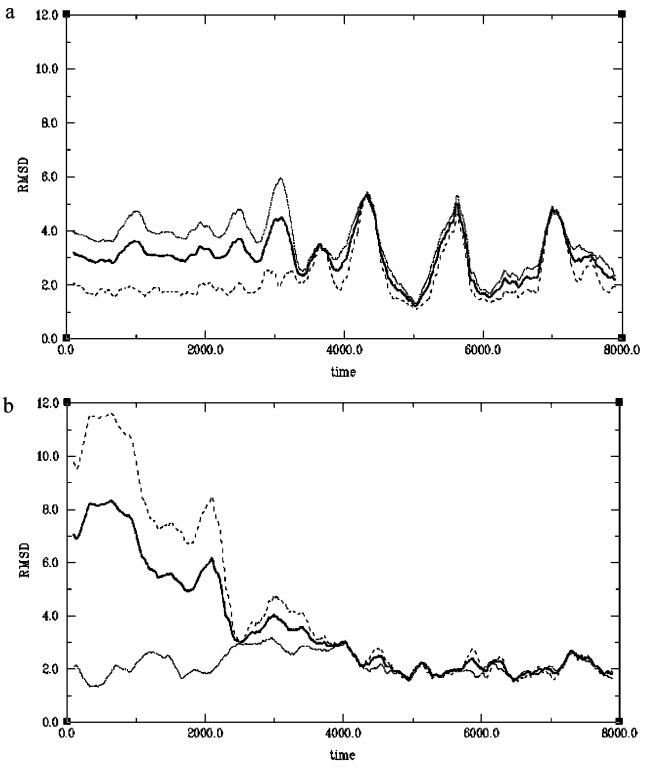

FIGURE 6. Representation of the heavy-atom positional root-mean-square deviation (Å) along the trajectories (ps) collected for models (a) **I** and (b) **II** in DMSO for the rotaxane system (solid) and the axle (dotted) and wheel (dashed) components. The RMSD was calculated by fitting the isophthaloyl unit of the axle. Contributions arising from the capping groups of the axle and *tert*-butyl groups in the wheel were not considered to reduce the statistical noise due to their fluctuations. Values determined by using the snapshots at 5 ns as reference structures.

conformation as the temperature is lowered. Particularly, the structural details of the co-conformation represented by model **I** agrees with the available experimental NMR data, such as the proximity of the isophthaloyl H_a proton to the wheel NH and H_A protons (around 2.8 Å) or the fact that the H_c proton lies at contact distances (around 2.9 Å) from the crown ether hydrogens (see Figure 1 for nomenclature). For the sake of comparison, a similar analysis for the model **II** structures revealed similar contact distances for H_c, but sensibly larger distances (>5 Å) for the contacts involving H_a.

Rotaxane in DMSO Solution. To examine the influence of the solvent on the conformational preferences of the rotaxane, a series of MD simulations in DMSO were performed using the same initial co-conformations of the [2]rotaxane (models **I**−**IV**).

For model **I**, the RMSD profile showed several transitions along the whole trajectory (Figure 6a). In the case of model **II**, there was a structural transition starting at around 1 ns and lasting for 3 ns until a new, stable structure, which persisted along the rest of the simulation, was achieved (Figure 6b). Finally, no remarkable structural fluctuations were observed in the RMSD profiles obtained for simulations of models **III** and **IV** (data not shown). As was found in chloroform, the PCA results allowed us to identify a partial circumrotation motion in the trajectory of model **II**, as noted in the global

TABLE 3. Global Similarity Index, Heavy-Atom Positional Root-Mean-Square Deviations (Å), and Energy Analysis (kcal/mol) for the Snapshots Collected in the Different Simulations of the Rotaxane in DMSO[a]

model	**I**	**II**	**III**	**IV**
	Global Similarity Index			
β	0.01	0.64	0.05	0.07
	RMSD			
	[5−8] ns	[5−8] ns	[5−8] ns	[5−8] ns
whole	**2.9**	**2.0**	**1.6**	**1.9**
axle/wheel	3.1/2.8	2.0/2.1	1.9/1.1	2.4/1.3
	Energy Analysis			
E_{axle}	118.7	121.5	119.8	120.9
	0.0	*+2.8*	*+1.1*	*+2.2*
E_{wheel}	178.6	179.1	180.3	185.3
	0.0	*+0.5*	*+1.7*	*+6.7*
$E_{axle-wheel}$				
vdW	−36.6	−32.1	−29.7	−38.6
ele	−0.6	−0.2	−0.2	−0.5
total	−37.2	−32.3	−29.9	−39.1
	0.0	*+4.9*	*+7.3*	*−1.9*
$\Delta E_{rotaxane}$	*0.0*	*+8.2*	*+10.1*	*+6.9*
$\Delta G_{s,ele}$	−20.6	−22.4	−21.8	−21.7
	0.0	*−1.8*	*−1.2*	*−1.1*
$\Delta G_{s,n-ele}$	−9.0	−9.6	−9.8	−8.9
	0.0	*−0.6*	*−0.8*	*+0.1*
$\Delta\Delta G_{s,total}$	*0.0*	*−2.4*	*−2.0*	*−1.0*
$-TS_{\infty}$	−105.6	−108.1	−99.4	−102.5
	0.0	*−2.5*	*+6.2*	*+3.1*
ΔG_{DMSO}	*0.0*	*+3.3*	*+14.3*	*+9.0*

[a] See footnote in Table 2. Relative values are given in italics using model I as reference system.

similarity index of 0.64 (see Table 3). In contrast, the index β was close to 0 for the rest of models.

Compared to the simulation in chloroform, no stable hydrogen-bond contact was found between the axle C═O and wheel NH groups in model **I**. In fact, a DMSO molecule is typically found above the axle isophthaloyl unit with the S═O group pointing toward the wheel NH groups. This finding agrees with the experimental evidence that a DMSO molecule can bind deeply within the cavity of the macrobicycle wheel, and even strongly compete with the binding of chloride anions.[8] The axle C═O group points toward the hydrogens of one of the aryl rings bound to the wheel's 1,3-dicarboxamide unit (Figure 7a). The transitions found in the RMSD profile stem from changes in the orientation of the C═O group, which forms (C)O···H(aryl) contacts with each of the hydrogens of the vicinal arene ring (Figure 7b), and by torsional fluctuations (in cases as large as 80°) around the C(═O)-O and O−C(aryl) bonds of the ester group more distant from the wheel. In contrast with the small fluctuations found for model **I**, the circumrotation motion in model **II** changes the relative position of axle and wheel by around 90 degrees (see Figure 7c,d). For model **III**, no stable hydrogen-bond contact was observed. Nevertheless, a weak hydrogen-bond between the axle C═O and one of the wheel NH groups that persisted along the simulation was observed for model IV (average (C═)O···H(N) distance of 3.1 Å in the [5−8] ns region; for the sake of comparison, the average (C═)O···H(N) distance in model **III** was generally larger than 4.5 Å).

A structural and energetic analysis of the different models was performed for the co-conformations sampled in the [5−8] ns windows. In all cases the *self* RMSD values are small and comparable to those reported for

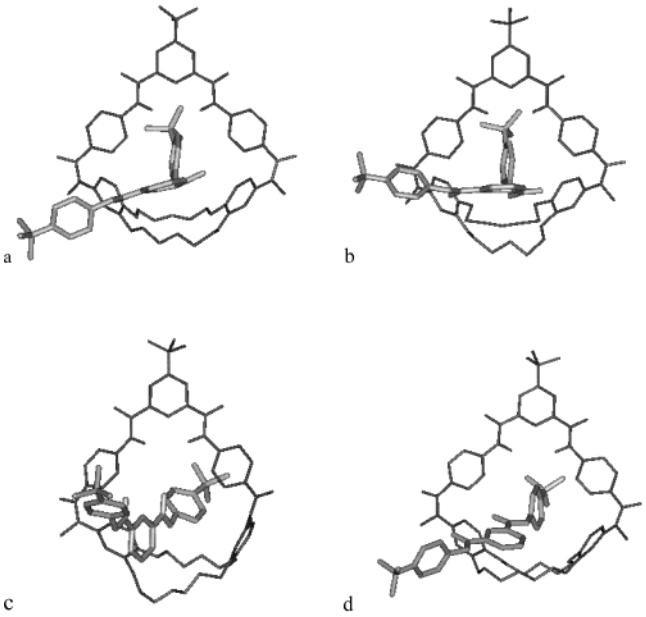

FIGURE 7. Representation of the snapshots collected at (a) 4 and (b) 6 ns for the trajectory of model **I** and at (c) 2 and (d) 5 ns for the trajectory of model **II** in DMSO. For the sake of clarity the capping groups of the axle and most of the hydrogens atoms are omitted.

the simulations in chloroform (see Table 3). Compared to model **I**, the internal energy of the rotaxanes destabilize models **II**−**IV** by 7−10 kcal/mol (see Table 3), an energy difference similar to that found for the rotaxane models in chloroform. Again, the energetic preference of model **I** mainly stems from the van der Waals term, but for model **IV**, where the maintenance of the (C═)O···H(N) contact (see above) is likely related to the increased strain in the wheel. Solvation in DMSO disfavors model **I** by 1−2 kcal/mol, a difference similar to that found in chloroform, though it mainly stems from the electrostatic term. Finally, the configurational entropy favors model **II**, but the difference with regard to model **I** is smaller than that found in chloroform. As a result, the structures sampled for model **I** are expected to be the main co-conformation of the rotaxane in DMSO. Overall, the free energy differences in DMSO (ΔG_{DMSO}; Table 3) indicates that the structures sampled for models **III** and **IV** are largely destabilized (by more than 9 kcal/mol) with regard to model **I**, which is predicted to be the main co-conformation in DMSO. Keeping in mind the uncertainty of the energy contributions, particularly the configurational entropy, the relative stability of model **II** (around 3 kcal/mol) do not allow us to exclude a significant population of this latter co-conformation in DMSO.

In summary, the preceding results indicate that the gross structural and energetic features of the rotaxane models are similar in both chloroform and DMSO. The most remarkable difference in the two solvents, however, concerns the lack of a hydrogen bond between the wheel NH and axle C═O groups for model **I** in DMSO, which can be explained by the higher permittivity and well-known hydrogen-bonding acceptor properties of DMSO.[30]

(30) (a) Catalán, J.; López, V.; Pérez, P.; Martín-Villamil, R.; Rodríguez, J. G. *Liebigs Ann.* **1995**, 241. (b) Catalán, J.; Díaz, C.; López, V.; Pérez, P.; de Paz, J. L. G. *Liebigs Ann.* **1996**, 1785.

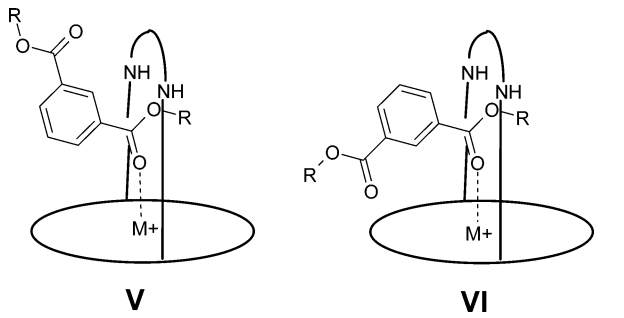

FIGURE 8. Schematic representations of the cation-bound rotaxane models **V** and **VI**.

The rotaxane model **I** in DMSO adopts a different co-conformation, where the axle C═O faces the aryl units of the wheel. However, the folded arrangement of the axle in model **I** (where the angle between the capping groups and the center of the isophthaloyl ring is around 120 degrees) inhibits large dynamical motions such as circumrotation, which are more likely when the axle adopts an extended orientation, as found in model **II**. Because trapping of the axle through hydrogen bonding between C═O and NH groups is more difficult in DMSO, the co-conformations are "less symmetrical" than in chloroform with the axle experiencing large changes in anisotropic shielding, which would explain why the NMR signals in DMSO are broadened.[11]

Rotaxane−Cation Complex in DMSO. To investigate the effect of cation binding on the structural behavior of the rotaxane in DMSO, a Na^+ cation was inserted within the crown ether and fixed at that position by suitable positional restrains. These restrains allow us to account for the relatively weak binding of the cation to the crown in DMSO and the consequent need to use a higher cation concentration in the experimental analysis (cation:rotaxane stoichiometry of 5:1).[11] Two different models were considered for the cation-bound rotaxane (see Figure 8). In the two models one of the axle C═O groups points toward the cation. Nevertheless, they differ in the orientation of the isophthaloyl unit, since the proton H_a is oriented toward the wheel NH groups (model **V**) or the wheel crown ether (model **VI**). Moreover, the ester group distal to the wheel was required to adopt a trans (**V**) or cis (**VI**) orientation relative to the proximal one, respectively, because other arrangements give rise to a largely steric clash between axle and wheel.

Inspection of the RMSD profile for model **V** revealed a marked structural transition at around 6 ns that lasts for around 0.5 ns (see Figure 9a), whereas several small fluctuations were observed for model **VI** (Figure 9b). The small values of the global similarity index β (see Table 4) rule out the involvement of any circumrotation motion, as expected from the tight interaction with the cation (the (C═)O···Na^+ distance was in the range 2.6−3.0 Å). The transition for model **V** was mainly due to a rotation around the (C═)O−O and O−C(aryl) bonds of the ester group bound to the cation, which changes their values from around 120 and 180° in the [1−4] ns window to −120 and 30° in the [11−14] ns one. As a result, the isophthaloyl proton H_a, which was pointing toward the aryl rings attached to the wheel dicarboxamide unit, changes its orientation and points toward the other wheel aryl ring after the transition (see Figure 10a,b). For

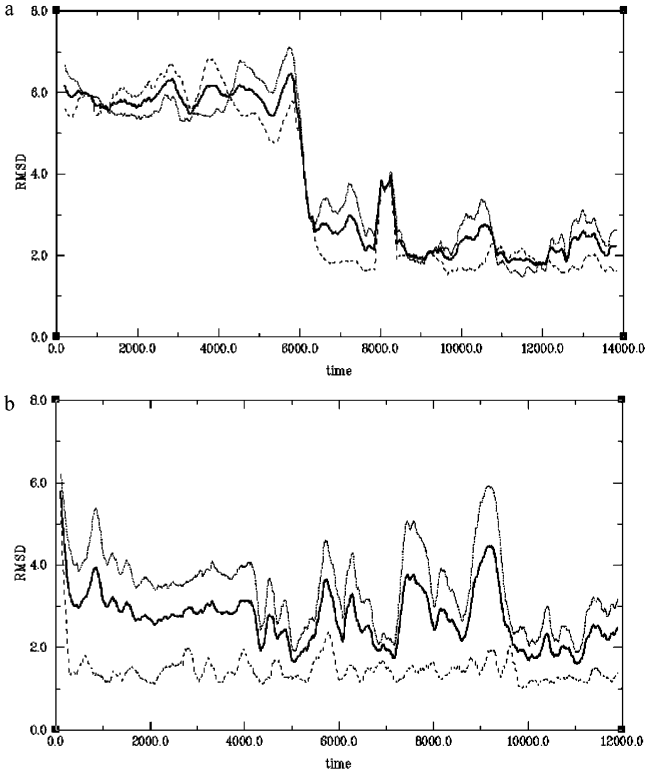

FIGURE 9. Representation of the heavy-atom positional root-mean-square deviation (Å) along the trajectories (ps) collected for the cation-bound models (a) **V** and (b) **VI** in DMSO for the rotaxane system (solid) and the axle (dotted) and wheel (dashed) components. The RMSD was calculated by fitting the isophthaloyl unit of the axle. Contributions arising from the capping groups of the axle and *tert*-butyl groups in the wheel were not considered to reduce the statistical noise due to their fluctuations. Values determined by using the snapshots at 11 (**V**) and 5 (**VI**) ns as reference structures.

model **VI**, the fluctuations mostly affected the (C═)O−O and O−C(aryl) bonds of the ester group not involved in the interaction with the cation, but they did not alter the orientation of the isopthaloyl unit (see Figure 10c,d).

Based on the RMSD profiles, the structural and energetic analysis of the two models was performed for the structures collected in the [1−4] and [11−14] ns windows for model **V** and [5−8] and [9−12] ns for model **VI**. The *self* RMSDs are similar to those obtained for the models of the free rotaxane in both chloroform and DMSO (see Table 4). Compared to the results found for the simulations of the free rotaxane in DMSO, the wheel NH groups were not observed to interact directly with a solvent molecule. This difference is due to the different orientation of the isophthaloyl unit, since the interaction of the axle C═O with the cation forced the isophthaloyl unit to be oriented perpendicular to the crown ether in the cation-bound rotaxane.

The internal energies of axle and wheel are comparable to the values obtained for the free rotaxane in DMSO, which implies that binding of the cation does not induce strain into the two components (see Table 4). The interaction energy between axle and wheel is similar in models **V** and **VI** and smaller than that found in the free rotaxane. The free energy of solvation of the rotaxane is similar for the two models and comparable to the values reported for the free rotaxane. The configurational entropy is smaller (in absolute value) for the cation-bound rotaxane than for the free rotaxane, as expected from the restricted flexibility due to the interaction with the cation. Nevertheless, it still favors the model where the axle adopts a more extended orientation (model **VI**) by around 3 kcal/mol.

TABLE 4. Global Similarity Index, Heavy-Atom Positional Root-Mean-Square Deviations (Å) and Energy Analysis (kcal/mol) for the Snapshots Collected in the Different Simulations of the Rotaxane−Sodium Cation Complex in DMSO[a]

model	**V**		**VI**	
	Global Similarity Index			
β	0.04		0.05	
	RMSD			
	[1−4] ns	[11−14] ns	[5−8] ns	[9−12] ns
whole	**2.3**	**2.2**	**2.8**	**3.0**
axle/wheel	2.4/2.2	2.4/2.0	3.5/1.5	4.1/1.4
	Energy Analysis			
E_{axle}	118.6		118.9	
	0.0		*+0.3*	
E_{wheel}	179.2		178.8	
	0.0		*−0.4*	
$E_{axle-wheel}$				
vdW	−32.9		−32.3	
ele	+2.0		+1.9	
total	−30.9		−30.4	
	0.0		*+0.5*	
$\Delta E_{rotaxane}$	*0.0*		*+0.4*	
$\Delta G_{s,ele}$	−21.6		−21.8	
	0.0		*−0.2*	
$\Delta G_{s,n-ele}$	−9.6		−9.7	
	0.0		*−0.1*	
$\Delta\Delta G_{s,total}$	*0.0*		*−0.3*	
$-TS_{backbone}$	−92.4		−95.8	
	0.0		*−3.4*	
ΔG_{DMSO}	*0.0*		*−3.4*	

[a] See footnote in Table 2. Relative values are given in italics using model **V** as reference system.

The preceding analysis indicates that model **VI** is the most plausible co-conformation of the cation-bound rotaxane in DMSO, though a significant fraction of the structures found for model **V** cannot be ruled out keeping in mind the uncertainty of the energetic contributions. For model **VI**, the isophthaloyl proton H_a is at van der Waals distances from the crown ether hydrogens, with distances close to 2.2 Å. Moreover, the two protons H_b are not equivalent, as only one of them remains close to the one of the wheel aryl rings, the interproton separation being as short as 2.0 Å. In case of model **V**, the isophthaloyl proton H_a is at close distances (between 2.1 and 2.6 Å) from the hydrogens of the two aryl rings attached to the dicarboxamide unit. Indeed, only one of the two protons H_b of the axle isophthaloyl unit is close to the crown ether hydrogens. These structural details would, therefore, agree with the experimentally observed cross-relaxation of the axle protons H_a and H_b with the protons of the wheel crown ether and aryl rings.[11] As can be seen in Figure 10, the natural fluctuations in the cation-bound rotaxane mainly arise from conformational changes in the axle, which can involve even the ester group that participates in the binding of the cation.

Summary and Final Remarks

Rotaxanes constitute a chemical framework suitable for making molecules in which *controlled* motions, such

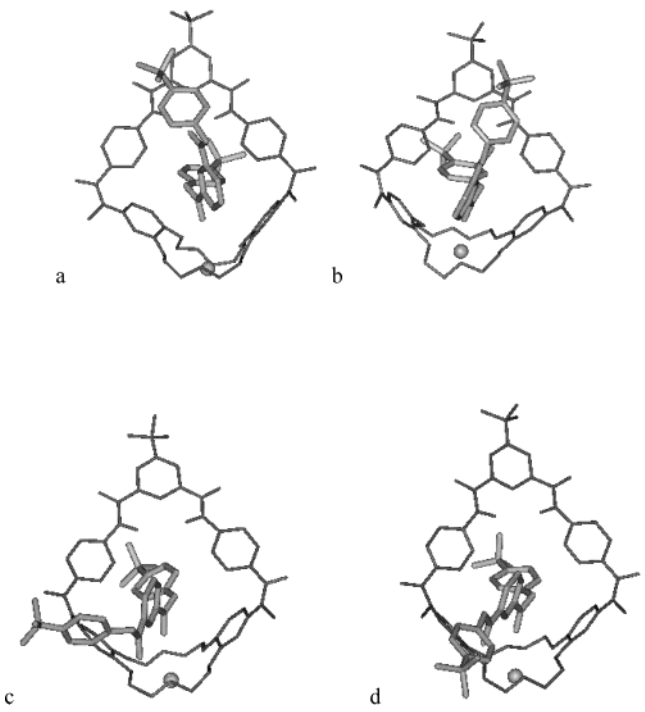

FIGURE 10. Representation of the snapshots collected at (a) 1 and (b) 11 ns for the trajectory of model **V** and at (c) 8 and (d) 9 ns for the trajectory of model **VI** in DMSO. The sphere denotes the location of the sodium cation. For the sake of clarity the capping groups of the axle and most of the hydrogens atoms are omitted.

as shuttling or circumrotation, occur. Equally important is the design of *switches* to control such motions. A number of switching strategies based on chemical, photochemical, and electrochemical effectors have been explored in recent years.[4−7] However, it is difficult to obtain a precise understanding of how these effectors influence the motions of the rotaxane components at the molecular scale. Despite the short time scale of the MD simulations reported here, the preceding results provide some clues about the influence of specific noncovalent factors on the structure and dynamics of the [2]rotaxane system shown in Figure 1.

In chloroform, a significant fraction of the rotaxane molecules are expected to have a hydrogen-bond contact between the axle C═O and wheel NH groups (Figure 5a,b). Such a co-conformation is in agreement with the available room-temperature ^{1}H NMR spectra,[11] which exhibit no apparent dynamic behavior upon cooling to −60 °C. Solvation in DMSO, however, breaks these hydrogen bonds and the rotaxane adopts a series of co-conformations, where the axle C═O faces the aryl units of the wheel and forms weak, transient (C)O···H(aryl) hydrogen bonds. The axle in these exchanging co-conformations experiences large changes in anisotropic shielding which explains why the NMR signals are broadened in DMSO.[11] Co-conformational exchange in DMSO is severely restricted upon insertion of a Na^+ cation into the crown ether and coordination to the ester C═O group. Under these circumstances, the rotaxane prefers a single co-conformation, which still allows some degree of rotational flexibility in the axle.

From a dynamic point of view, several experimental studies have identified large-amplitude motions in related rotaxane structures that occur in a time-scale longer than 10^{-6} s^{-1} at ambient temperature.[31] Specifically, free energy barriers for the macrocycle rotation about the axle ranging from 11 to 15 kcal/mol have been reported.[31b,c] Although the MD simulations reported here are too short to characterize completely such motions, the study has shown that the natural fluctuations of the [2]rotaxane can produce partial circumrotation motions in a few nanoseconds. Circumrotation is facilitated in less hindered rotaxane co-conformations, particularly when the axle is extended in a perpendicular orientation to the wheel.

On the basis of the structural and energetic analysis discussed above, it appears that circumrotation of the rotaxane is the result of a series of dynamic processes. The first process is an axle sliding step that breaks the hydrogen bonds between the axle C═O and the wheel NH groups; this can be viewed as a molecular switch that is able to control co-conformational movements in the rotaxane. The second step is a circumrotation step where circumrotation of the axle relative to the wheel progresses through a series of weak, transient contacts between the axle C═O group and the hydrogens of the wheel aryl rings. This circumrotation step is facilitated when the axle is in an extended conformation. In other words, internal rotation around the (O═)C···C(isophthaloyl) bond of the axle ester group distal to the wheel affects circumrotation by converting a folded axle conformation to a less hindering extended one. This latter factor is expected to be of particular relevance owing to the partial double-bond character of the (O═)C···C(aryl) bond, which gives rise to barriers in the range 6−11 kcal/mol and coalescence temperatures varying from −142 to −56° depending on exact structure.[32] While the two previous dynamic processes can be influenced by external, noncovalent factors such as the nature of the solvent or the addition of salts, the third factor opens the possibility of controlling the dynamics of the [2]rotaxane co-conformation by modulating the internal flexibility of the axle through covalent attachment of suitable functional groups.

Acknowledgment. We are grateful to Prof. W. L. Jorgensen for a copy of his BOSS program and Prof. J. Tirado-Rives for a copy of the SURFPDB program. We thank the Ministerio de Ciencia y Tecnología for financial support (Grant Nos. SAF2002-04282 and PM99-0046), the US National Science Foundation, and the Centre de Supercomputació de Catalunya for computational facilities.

JO034457D

(31) (a) Leigh, D. A.; Murphy A.; Smart, J. P.; Slawin, A. M. Z. *Angew. Chem., Int. Eng. Ed.* **1997**, *36*, 728. (b) Ashton, P. R.; Bravo, J. A.; Raymo, F. M.; Stoddart, J. F.; White, A. J. P.; Williams, D. J. *Eur. J. Org. Chem.* **1999**, 899. (c) Bermudez, V.; Capron, N.; Gase, T.; Gatti, F. G.; Kajzar, F.; Leigh, D. A.; Zxerbetto, F.; Zhang, S. *Nature* **2000**, *406*, 608

(32) (a) Anet, F. A. L.; Ahmad, M. *J. Am. Chem. Soc.* **1964**, *86*, 119. (b) Kessler, H. *Angew. Chem., Int. Ed. Engl.* **1970**, *9*, 219.